

Interactions between Organized, Surface-Confined Monolayers and Liquid-Phase Probe Molecules. 3. Fundamental Aspects of the Binding Interaction between Charged Probe Molecules and Organomeraptan Monolayers

Todd A. Jones,[†] Gregory P. Perez,[†] Bryan J. Johnson,[‡] and Richard M. Crooks^{*,†}

Department of Chemistry, Texas A&M University, College Station, Texas 77843-3255, and Department of Chemistry, University of New Mexico, Albuquerque, New Mexico 87131

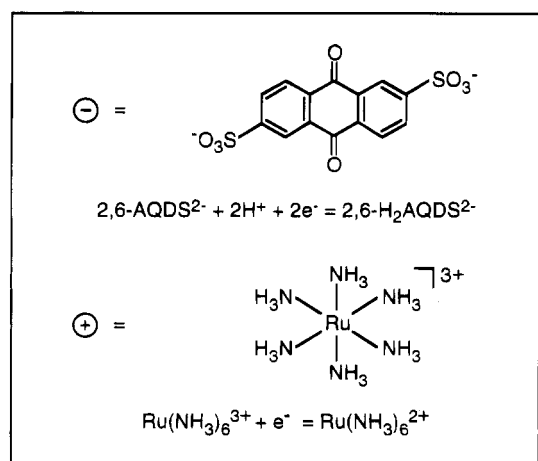
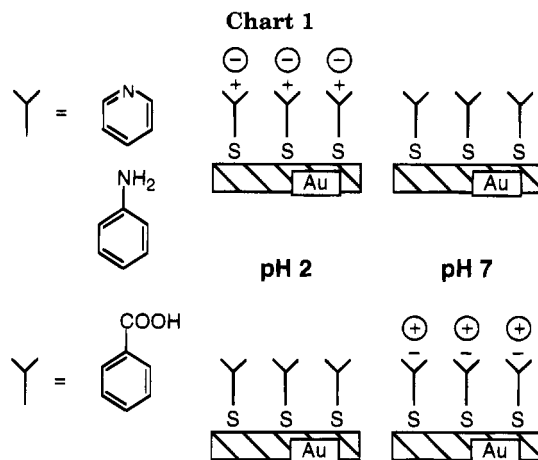
Received August 25, 1994. In Final Form: January 9, 1995[⊗]

We report that Au electrodes modified with monolayers of functionalized organomeraptan derivatives show a pH-dependent electrostatic binding interaction with oppositely charged probe molecules. The extent of binding is discussed in terms of the position of the charge on the organic surface, the magnitude and distribution of the charge on the probe, the probe concentration, the degree of surface protonation, and intermolecular interactions between the organomeraptan monolayer and the electrolyte ions. Specifically, we examined the interaction between a series of sulfonated anthraquinone probe molecules, anthraquinone-2,6-disulfonic acid (2,6-AQDS²⁻), anthraquinone-1,5-disulfonic acid, and anthraquinone-2-sulfonic acid, and surface-confined isomers of mercaptopyridine. 4-Mercaptopyridine and 2-mercaptopyridine monolayers dramatically alter the molecular adsorption characteristics of Au surfaces. For example, at low pH, when the surface-confined mercaptans are protonated, they bind sulfonated anthraquinones, but at high pH, when the monolayer is deprotonated and electrically neutral, no binding occurs. Quinones bound to the mercaptopyridine surfaces can be released by changing the pH of the phosphate buffer from acidic to neutral pH. We also find that probe molecules having multiple binding sites interact most strongly with the 4-mercaptopyridine surface, that the surface concentration of adsorbed 2,6-AQDS²⁻ increases as its bulk-phase concentration increases, and that increasing the concentration of electrolyte decreases the surface concentration of adsorbed 2,6-AQDS²⁻.

Introduction

In this paper we report results relevant to the chemical and structural basis of pH-dependent electrostatic binding between liquid-phase ions and Au surfaces modified with single layers of organomeraptans.¹ Our results indicate the following variables are important in pH-dependent electrostatic binding of molecules to monolayer surfaces: (1) the position of the functional groups of the surface-confined molecules that are responsible for the binding interaction; (2) the number of charges on the probe ion; (3) the solution concentration of the probe; (4) the concentration and types of ions that compete with the redox probe for surface binding sites; (5) the extent of monolayer protonation; (6) intermolecular forces other than those arising from pure ion-ion interactions.

Chart 1 illustrates the principle of electrostatic binding of liquid-phase probe molecules to surface-confined monolayers. Basic functional groups, such as pyridine or aniline, are deprotonated at high pH and negatively charged probe molecules do not electrostatically bind to the organomeraptan-modified surface; however, at low pH the surface is positively charged and the probe undergoes specific adsorption. For example, we have previously reported that Au surfaces modified with 4-aminothiophenol (4-ATP) selectively bind solution-phase redox probe molecules, such as anthraquinone-2,6-disulfonic acid (2,6-AQDS²⁻), as a function of solution pH: at low pH, 4-ATP is protonated and binds 2,6-AQDS²⁻, but at high pH 4-ATP deprotonates and 2,6-AQDS²⁻ is released.¹ Neutral or positively charged molecules are not bound to a significant degree at any pH. Carboxylic



* Author to whom correspondence should be addressed.

[†] Texas A&M University.

[‡] University of New Mexico.

[⊗] Abstract published in *Advance ACS Abstracts*, March 1, 1995.

(1) Sun, L.; Johnson, B. J.; Wade, T.; Crooks, R. M. *J. Phys. Chem.* **1990**, *94*, 8869.

acid-functionalized monolayer surfaces exhibit the opposite pH dependence: at high pH, the acid is deprotonated

and positively charged ions adsorb to the negatively charged surface, but at low pH the organic surface is electrically neutral and electrostatic binding is not possible.² Here, we focus on surface-confined bases, but in the fifth paper in this series we will discuss electrostatic binding by acid surfaces.²

Monolayer surfaces that undergo specific interactions with molecules have important applications as components in molecular-recognition-based chemical sensors and as model surfaces for a range of boundary-layer phenomena including those associated with adhesion, lubrication, and biological studies. To implement such applications, however, it is essential to develop a complete understanding of monolayer/molecule interactions. Therefore, we have previously used the general approach shown in Chart 1 to investigate several types of intermolecular interactions other than those resulting primarily from electrostatic interactions; these include covalent bonding, complexation and acid-base interactions, and hydrogen bonding.³

Our initial report of electrostatic binding of ions by organized monolayer surfaces¹ was predated by a large body of related research. The first and most conceptually-related experiments were performed by Anson and co-workers,⁴ who modified electrode surfaces with pH-sensitive polymers, such as poly(4-vinylpyridine) or poly(acrylic acid), that contain either covalently-linked positively or negatively charged ionic groups depending on the solution pH. When polymer-modified surfaces such as these are immersed in a solution at the proper pH, solution-phase metal-ion complexes of opposite charge, such as IrCl_6^{3-} or $\text{Ru}(\text{NH}_3)_6^{3+}$, preferentially and persistently partition into the polymer. This electrostatic trapping of electroactive ions in polymers is closely related to ion-exchange methods used in separation science. Other studies by Anson's group showed that similar phenomena occur when polymers containing pH-independent permanent charges, such as quaternized poly(4-vinylpyridine), poly(vinyl sulfate), or poly(styrenesulfonate), are used to adsorb ions. Many other combinations of electroinactive or electroactive polymers that electrostatically bind electrochemically active ions have been reported; a complete discussion of the electrochemical aspects of ion binding by polymer films is provided in the excellent review by Murray.⁵

Monolayer surfaces that electrostatically bind ions and ionic polymers have also been reported. For example, in addition to our own reports,^{1,3c} this general approach has been used by Bowden and co-workers⁶ to show that cytochrome *c* adsorbs to carboxylic acid-terminated self-

assembled monolayers (SAMs). Sagiv has recently shown that electrostatic binding can be used to build-up organized multilayer structures,⁷ and Decher and co-workers⁸ have shown that organized layers of ionic polymers can be constructed using a sequential layering technique based on electrostatic interactions. Corn *et al.* have demonstrated a similar principle by electrostatically binding poly-L-lysine to an acid-terminated SAM.⁹ The extensive literature on ion binding by polymer-modified surfaces has focused primarily on catalysis, charge trapping, and other aspects of mass and electron transfer.⁵ In these previous studies, it was generally assumed that only, or at least primarily, electrostatic interactions were responsible for ion binding. However, since the polymers used in these studies were thick and amorphous, and since no good analytical techniques are available to study the microstructure of such systems, it has been impossible to definitively and quantitatively describe the specific nature of intermolecular interactions that give rise to the observed behavior. In contrast to polymeric media, SAMs provide excellent model environments for studying interactions between analytes and organic surfaces, since they are highly ordered and their average properties, which are thought to strongly reflect their nanoscopic properties, are easily characterized both *in situ* and *ex situ*.¹⁰⁻¹²

The principal focus of the present series of articles^{1,2,13} is to examine fundamental aspects of intermolecular interactions between surface-confined organic molecules and simple liquid-phase probe molecules by taking advantage of the structurally and chemically well-ordered SAM environment. This approach lifts much of the structural ambiguity and complicated mass- and electron-transfer phenomena associated with thick, amorphous organic modifiers, since it is now well established that exactly one monolayer of certain organomeraptans specifically adsorb to Au surfaces.¹¹ Moreover, depending on the degree of substrate crystallinity and the magnitude of intramonolayer chemical interactions, which can arise through van der Waals, covalent, or hydrogen-bonding interactions,³ SAMs may display a high degree of two-dimensional structure. In the present work, we have made an effort to use previously studied SAMs, which we know from scanning tunneling microscopy studies reproducibly form at least partially-ordered monolayers.¹⁴ However, we have not quantitatively examined the structures of

(2) Jones, T. A.; Perez, G. P.; Crooks, R. M. Manuscript in preparation.

(3) (a) Thomas, R. C.; Sun, L.; Crooks, R. M.; Ricco, A. J. *Langmuir* **1991**, *7*, 620. (b) Sun, L.; Thomas, R. C.; Crooks, R. M.; Ricco, A. J. *J. Am. Chem. Soc.* **1991**, *113*, 8550. (c) Kopley, L. J.; Crooks, R. M.; Ricco, A. J. *Anal. Chem.* **1992**, *64*, 3191. (d) Sun, L.; Crooks, R. M.; Ricco, A. J. *Langmuir* **1993**, *9*, 1775. (e) Xu, C.; Sun, L.; Kopley, L. J.; Crooks, R. M.; Ricco, A. J. *Anal. Chem.* **1993**, *65*, 2102. (f) Crooks, R. M.; Xu, C.; Sun, L.; Hill, S.; Ricco, A. J. *Spectroscopy* **1993**, *8*, 28. (g) Thomas, R. C.; Tangyunong, P.; Houston, J. E.; Michalske, T. A.; Crooks, R. M. *J. Phys. Chem.* **1994**, *98*, 4493. (h) Ricco, A. J.; Crooks, R. M.; Xu, C.; Allred, R. E. In *Interfacial Design and Chemical Sensing*; Harrison, D. J., Mallouk, T. E., Eds.; ACS Symposium Series 561; American Chemical Society: Washington, DC, 1994; Chapter 23. (i) Crooks, R. M.; Chailapakul, O.; Ross, C. B.; Sun, L.; Schoer, J. K. In *Interfacial Design and Chemical Sensing*; Harrison, D. J., Mallouk, T. E., Eds.; ACS Symposium Series 561; American Chemical Society: Washington, DC, 1994; Chapter 10.

(4) (a) Oyama, N.; Anson, F. C. *J. Electrochem. Soc.* **1980**, *127*, 247. (b) Oyama, N.; Anson, F. C. *Anal. Chem.* **1980**, *52*, 1192. (c) Oyama, N.; Shimomura, T.; Shigehara, K.; Anson, F. C. *J. Electroanal. Chem.* **1980**, *112*, 271. (d) Shigehara, K.; Oyama, N.; Anson, F. C. *Inorg. Chem.* **1981**, *20*, 518.

(5) Murray, R. W. In *Electroanalytical Chemistry*; Bard, A. J., Ed.; Marcel Dekker: New York, 1984; Vol. 13, pp 330-333.

(6) (a) Tarlov, M. J.; Bowden, E. F. *J. Am. Chem. Soc.* **1991**, *113*, 1847. (b) Collinson, M.; Bowden, E. F.; Tarlov, M. *J. Langmuir* **1992**, *8*, 1247. (c) Reeves, J. H.; Song, S.; Bowden, E. F. *Anal. Chem.* **1993**, *65*, 683. (d) Song, S.; Clark, R. A.; Bowden, E. F.; Tarlov, M. *J. Phys. Chem.* **1993**, *97*, 6564. (e) Nahir, T. M.; Clark, R. A.; Bowden, E. F. *Anal. Chem.* **1994**, *66*, 2595.

(7) Sagiv, J. The Weizmann Institute of Science, personal communication, 1994.

(8) (a) Decher, G.; Hong, J. D. *Makromol. Chem. Macromol. Symp.* **1991**, *46*, 321. (b) Decher, G.; Hong, J. D. *Ber. Bunsenges. Phys. Chem.* **1991**, *95*, 1430. (c) Decher, G.; Hong, J. D.; Schmitt, J. *Thin Solid Films* **1992**, *210/211*, 831. (d) Lvov, Y.; Decher, G.; M \ddot{o} hwald, H. *Langmuir* **1993**, *9*, 481. (e) Lvov, Y.; Essler, F.; Decher, G. *J. Phys. Chem.* **1993**, *97*, 13773. (f) Decher, G.; Lvov, Y.; Schmitt, J. *Thin Solid Films* **1994**, *244*, 772.

(9) Jordan, C. E.; Frey, B. L.; Kornguth, S.; Corn, R. M. *Langmuir* **1994**, *10*, 3642.

(10) (a) Bigelow, W. C.; Pickett, D. L.; Zisman, W. A. *J. Colloid Sci.* **1946**, *1*, 513. (b) Bigelow, W. C.; Glass, E.; Zisman, W. A. *J. Colloid Sci.* **1947**, *2*, 563.

(11) (a) Nuzzo, R. G.; Allara, D. L. *J. Am. Chem. Soc.* **1983**, *105*, 4481. (b) Bain, C. D.; Troughton, E. B.; Tao, Y. T.; Ewall, J.; Whitesides, G. M.; Nuzzo, R. G. *J. Am. Chem. Soc.* **1989**, *111*, 321, and references therein. (c) Dubois, L. H.; Nuzzo, R. G. *Annu. Rev. Phys. Chem.* **1992**, *43*, 437, and references therein.

(12) Ulman, A. *An Introduction to Ultrathin Organic Films*; Academic: New York, 1991.

(13) (a) Chailapakul, O.; Crooks, R. M. *Langmuir* **1993**, *9*, 884. (b) Chailapakul, O.; Crooks, R. M. *Langmuir*, **1995**, *11*, 0000.

(14) Bard, A. J., The University of Texas at Austin, personal communication, 1993.

Table 1. Bulk-Phase and Surface-Adsorbed Electrochemical Characteristics of the Probe Molecules Used in this Study^a

	pH 2			pH 7		
	E° (mV)	ΔE_p (mV)	$\Gamma_{2,6\text{-AQDS}^{2-}}$ (10^{-10} mol/cm ²)	E° (mV)	ΔE_p (mV)	$\Gamma_{2,6\text{-AQDS}^{2-}}$ (10^{-10} mol/cm ²)
Au/2,6-AQDS ²⁻ - _{bulk}	-163	225		-439	170	
Au/2,6-AQDS ²⁻ - _{ads}	-90	40	0.13	<i>b</i>	<i>b</i>	<i>b</i>
Au/1,5-AQDS ²⁻ - _{bulk}	<i>c</i>	<i>c</i>		-428	540	
Au/1,5-AQDS ²⁻ - _{ads}	<i>c</i>	<i>c</i>	<i>c</i>	<i>d</i> , $E_{p,c} = -205$	<i>d</i>	0.12
Au/2-AQMS ⁻ - _{bulk}	-195	254		-464	75	
Au/2-AQMS ⁻ - _{ads}	-173	62	0.05	-462	51	0.08

^a All results were obtained in 0.2 M phosphate buffer solutions containing 1.0 mM probe-molecule concentrations. The scan rates were 100 mV/s and the average true area of the electrodes was 0.27 cm². Data in this table are comparable to those in ref 1. Differences in surface concentrations arise from slight differences in the surface preparation technique and because here we take into account surface roughness. ^b $\Gamma_{2,6\text{-AQDS}^{2-}} < 0.04 \times 10^{-10}$ mol/cm². ^c Electrolyte solution reduction interferes with reduction of probe molecule. ^d Irreversible cyclic voltammetric wave.

either the mercaptan monolayers or the bilayer structures that result from electrostatic binding. This logical expansion of the work reported here will be described in subsequent papers in this series.

Experimental Section

Chemicals. The 4-mercaptopyridine (4-MP) was obtained from Aldrich (Milwaukee, WI) and purified either by vacuum sublimation or according to a literature procedure.¹⁵ The 2-mercaptopyridine (2-MP), 99%, was used as received from Aldrich. Anthraquinone-2,6-disulfonic acid, disodium salt (2,6-AQDS²⁻), anthraquinone-1,5-disulfonic acid, disodium salt (1,5-AQDS²⁻), and anthraquinone-2-sulfonic acid, monosodium salt (2-AQMS⁻) were obtained from Aldrich and recrystallized once from water using decolorizing charcoal. Buffer solutions were made from reagent-grade chemicals. Phosphate buffers, nominally pH 2 and 7, had an analytical phosphate concentration, $c_{\text{PO}_4^{3-}}$, of 0.2 M unless otherwise noted and were made from equimolar mixtures of H₃PO₄ and NaH₂PO₄ or NaH₂PO₄ and Na₂HPO₄, respectively. Water was purified using a Milli-Q filtering system (Millipore). All soaking solutions and the electrochemical cell were deoxygenated with N₂ and a blanket of N₂ was kept over the solution in the electrochemical cell during measurements. All of the quinone solutions were kept in the dark to prevent undesirable photochemical transformations.¹⁶ All solutions, except buffers, were prepared immediately prior to the experiments. The quinones and the 4-MP were repurified often to ensure low levels of decomposition products, which can interfere with electrostatic binding experiments.

Procedures. Immediately prior to modification, electrodes were cleaned by being immersed in freshly prepared "piranha" solution (3H₂SO₄:1H₂O₂, **Caution:** piranha solution reacts violently with organic compounds, and it should not be stored in closed containers), rinsed with water and then ethanol, and dried under a stream of N₂. Unless otherwise noted in the text, organomercaptan monolayers were formed by soaking 0.5-mm-diameter Au wires (99.994%, AESAR/Johnson Matthey), which had geometrically projected surface areas of 0.159 cm², in 1 mM ethanolic (McCormick Distillers, 100%) solutions of the mercaptans for 15 h. We determined the surface roughness of the electrodes using an iodide adsorption technique.¹⁷ The ratio of the true surface area to the geometrically projected area results in an average roughness factor of 1.7 ± 0.2 . Surface concentrations reported here are based on the average true surface area of the polycrystalline Au wires, which is 1.7 times larger than the geometrically projected area.

Surface concentration measurements were made as follows unless noted otherwise in the text. First, the organomercaptan-modified Au electrode was immersed in a 0.2 M buffer solution of the appropriate anthraquinone probe molecule (1 mM) at open circuit for 5 min. Second, the electrode was removed from the probe-molecule-containing solution, rinsed for 10 s by draining pure aqueous buffer solution contained in a 3-mL pipet over the

Au wire, and then immersed in a probe-molecule-free buffer solution. Unless otherwise noted, all values for surface concentrations were obtained from the first cyclic voltammetric scan, which was initiated exactly 30 s after transfer of the electrode from the quinone-containing solution to the pure buffer solution, and surface concentrations were determined by halving the integrated current under both the cathodic and anodic portions of the cyclic voltammetric peaks corresponding to the surface-confined probe molecule. We used this method in conjunction with an *in situ* background correction technique (*vide infra*) to minimize measurement errors and subtract capacitive currents.

Values for E° were obtained by averaging the potentials corresponding to the peak cathodic current, $E_{p,c}$, and peak anodic current, $E_{p,a}$. Cyclic voltammetric data were obtained by using a Pine Instrument Co. Model AFRDE4 potentiostat and a gas-tight, four-neck, round-bottomed electrochemical cell that contained either one or two Au working electrodes, a Pt-gauze counter electrode, and a Ag/AgCl (3 M NaCl) reference electrode (Bioanalytical Systems, Inc.). Data were recorded on a Kipp and Zonen Model BD91 X-Y recorder.

Results and Discussion

Electrochemistry of the Probe Molecules at Naked Au Surfaces. We used three different electrochemically-active quinone probe molecules to study the chemical characteristics of SAMs having basic terminal groups: anthraquinone-2,6-disulfonic acid (2,6-AQDS²⁻), anthraquinone-1,5-disulfonic acid (1,5-AQDS²⁻), and anthraquinone-2-monosulfonic acid (2-AQMS⁻). These three sulfonated anthraquinones remain negatively charged over the entire range of pH studied and they undergo a two-electron, two-proton reduction to the corresponding hydroquinones at low pH, or a two-electron, one-proton reduction to the semiquinone at intermediate pH (for 2,6-AQDS²⁻: $pK_{a,1} = 7.35$, $pK_{a,2} = 10.3$),¹⁸ as illustrated for 2,6-AQDS²⁻ in Chart 1.

We evaluated the surface- and bulk-phase electrochemistry of the three probe molecules at naked Au electrodes to contrast this behavior with that found for the SAM-modified surfaces (Table 1). The electrochemical behavior of 2,6-AQDS²⁻ (Figure 1a) is typical of all three quinones. To obtain these data, we cleaned a single Au wire with piranha solution, rinsed it with water, and placed it in a N₂-purged pH = 2 or 7 buffer solution. The resulting voltammetry for the naked Au electrode is shown on the left side of Figure 1a. Next we placed the electrode in a solution containing 1 mM 2,6-AQDS²⁻ and 0.2 M phosphate buffer for 3 min to obtain the voltammetry of bulk-phase 2,6-AQDS²⁻ (2,6-AQDS²⁻-_{bulk}, center of Figure 1a). To determine if any 2,6-AQDS²⁻ adsorbed to the naked Au surface, we removed the electrode from the 1 mM 2,6-AQDS²⁻, rinsed it with probe-molecule-free buffer, and then returned it to the original phosphate-buffer solution.

(15) Allen, P. M.; Hill, H. A. O.; Walton, N. J. *J. Electroanal. Chem.* **1984**, *178*, 69.

(16) He, P.; Crooks, R. M.; Faulkner, L. R. *J. Phys. Chem.* **1990**, *94*, 1135, and references therein.

(17) Rodriguez, J. F.; Mebrahtu, T.; Soriaga, M. P. *J. Electroanal. Chem.* **1987**, *233*, 283.

(18) Ksenzhek, O. S.; Petrova, S. A.; Oleinik, S. V.; Kokodyashnyi, M. V.; Moskovskii, V. Z. *Elektrokhimiya* **1977**, *13*, 182.

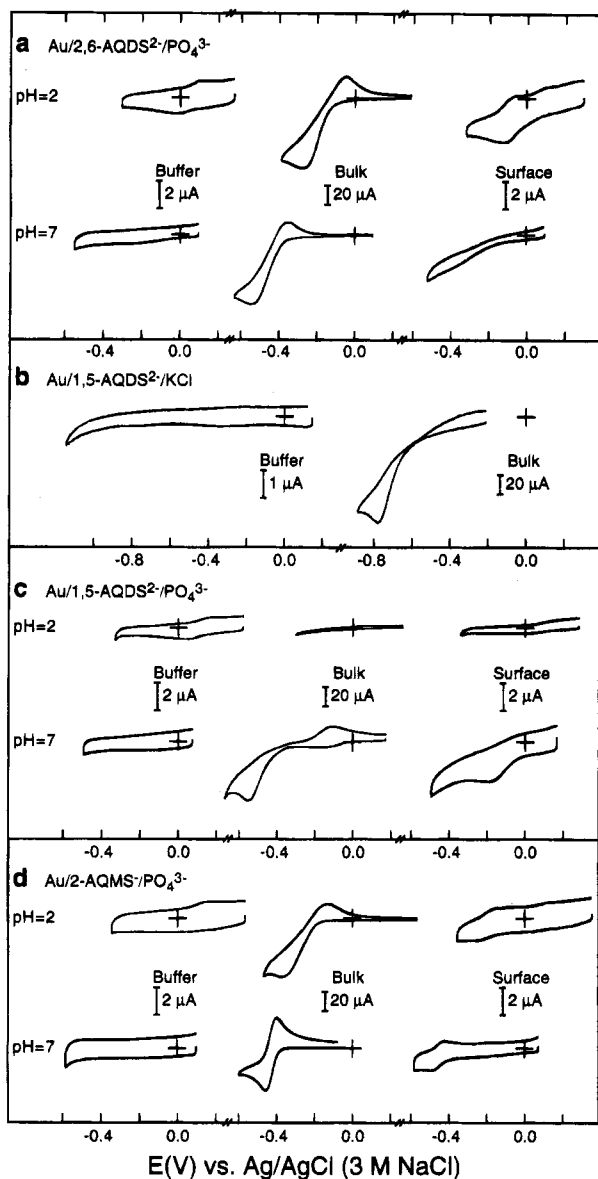


Figure 1. Cyclic voltammetry at naked Au electrodes: (a) 2,6-AQDS²⁻; (b and c) 1,5-AQDS²⁻; and (d) 2-AQMS⁻ showing bulk-phase and surface-adsorbed electrochemical characteristics. We determined surface concentrations of adsorbed probe molecules (Table 1) by integrating the Faradaic charge under the cathodic peaks of the voltammograms shown on the right side of the figure. The electrolyte concentration was 0.2 M and the scan rate was 100 mV/s. Other relevant information is given in the figure or in the Experimental Section.

The resulting voltammetry, which is shown on the right side of Figure 1a, is characteristic of 2,6-AQDS²⁻ adsorbed (2,6-AQDS²⁻_{ads}) to the naked Au surface. We repeated this process for each probe molecule at pH 2 and 7.

Cyclic voltammograms of the two buffer solutions indicate a low level of O₂ contamination after purging with N₂ for a few minutes. Although we found that prolonged purging with N₂ removed all traces of O₂, control experiments indicated that the level of O₂ indicated by the voltammograms does not affect the analysis of surface-confined 2,6-AQDS²⁻. The difference in the peak-current potentials, ΔE_p , for 2,6-AQDS²⁻_{bulk} indicates that the electron transfer is slow at low pH but somewhat more facile at elevated pH where the proton reactions are less important. For 2,6-AQDS²⁻_{ads} on the naked Au surface, ΔE_p is about 40 mV, which indicates faster electron-transfer kinetics. The $E^{o'}$ value for 2,6-AQDS²⁻_{ads} is about 70 mV positive of the bulk-phase value, which suggests

that reduced 2,6-AQDS²⁻ is more strongly adsorbed to the naked Au surface than the starting material.¹⁹ This result is consistent with a previously proposed model in which the reduced form of 2,6-AQDS²⁻ undergoes intermolecular hydrogen bonding on a clean Hg surface.¹⁶

The surface concentration of 2,6-AQDS²⁻_{ads}, $\Gamma_{2,6-AQDS^{2-}}$, is $(0.13 \pm 0.1) \times 10^{-10}$ mol/cm² (all surface concentrations take into account the surface roughness), much less than the theoretical value for a flat-adsorbed, close-packed monolayer, 1.3×10^{-10} mol/cm².^{20a} The concentration of 2,6-AQDS²⁻ in the soaking solution does not affect $\Gamma_{2,6-AQDS^{2-}}$ significantly. We were unable to confirm the presence of 2,6-AQDS²⁻_{ads} at pH = 7, although the voltammetry is somewhat different before and after immersion in the 2,6-AQDS²⁻ solution. The results of these control experiments are in general accord with previous reports for 2,6-AQDS²⁻ electrochemistry on Au,¹ Hg,¹⁶ Pt,²⁰ and highly-oriented pyrolytic graphite electrodes.²¹

We were not able to examine the electrochemistry of 1,5-AQDS²⁻_{bulk} at naked Au surfaces at pH = 2 (Figure 1c), since $E^{o'}$ lies beyond the polarizable limit of the phosphate buffer. We confirmed this finding by locating the 1,5-AQDS²⁻_{bulk} reduction wave in a KCl-containing electrolyte solution (Figure 1b). We observed the chemically and thermodynamically irreversible wave at $E_{p,c} = -0.78$ V, about 0.4 V beyond the onset of the Faradaic background process in the pH = 2 phosphate buffer. The reduction of 1,5-AQDS²⁻_{bulk} at pH = 7 indicates a thermodynamically irreversible process, and we observe a small and poorly defined surface electrochemical process at this pH. The bulk-phase and surface electrochemistry of 2-AQMS⁻ (Figure 1d) are similar to that of 2,6-AQDS²⁻. The principal difference concerns 2-AQMS⁻ surface adsorption, which is clearly detectable at both pH = 2 and 7.

For the purposes of this paper, the data in Figure 1 can be summarized as follows. The differences in the electrochemistry of these probe molecules are minimal at naked Au substrates. Except for 1,5-AQDS²⁻ at pH = 2, we observe both reduction and oxidation waves for each of the quinones. In addition, a small amount of the quinone adsorbs to the naked Au electrode. Specific details for all three probes are given in Table 1. The important result of this part of the study is that the SAMs dramatically change the molecular adsorption characteristics (*vide infra*) of the quinones and that the underlying Au surface exhibits a very minor influence on quinone adsorption behavior in the presence of SAMs.

Electrochemical Characteristics of the SAMs and the Quinone Probe Molecules. We performed several systematic experiments to determine the best conditions for obtaining a fundamental understanding of the interactions between liquid-phase quinone molecules and organomeraptan SAMs. Our results indicate that the most reproducible and easily interpretable data arise from 2,6-AQDS²⁻ adsorbed onto a 4-mercaptopyridine SAM (Au/4-MP/2,6-AQDS²⁻_{ads}). Therefore, we have focused this study on that particular system, but we will also discuss the other combinations of SAMs and probes in less detail.

The first set of experiments involves optimization of the experimental conditions required to achieve reproducible and limiting results. The relevant parameters

(19) Bard, A. J.; Faulkner, L. R. *Electrochemical Methods*; Wiley: New York, 1980; Chapter 12.

(20) (a) Soriaga, M. P.; Hubbard, A. T. *J. Am. Chem. Soc.* **1982**, *104*, 2735. (b) Soriaga, M. P.; Hubbard, A. T. *J. Am. Chem. Soc.* **1982**, *104*, 3937. (c) Hubbard, A. T. *Chem. Rev.* **1988**, *88*, 633, and references therein.

(21) McDermott, M. T.; Kneten, K.; McCreery, R. L. *J. Phys. Chem.* **1992**, *96*, 3124.

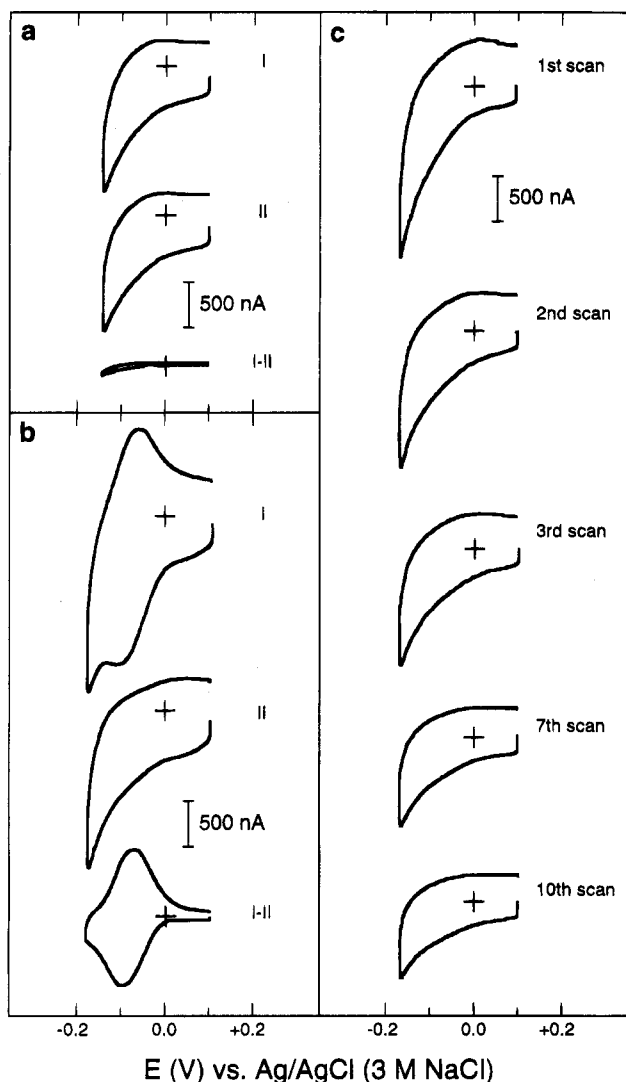


Figure 2. Cyclic voltammetry of (a) two electrodes modified simultaneously with 4-MP only (I and II), and the difference in the currents (I–II) obtained by real-time subtraction; (b) 2,6-AQDS²⁻ electrostatically bound to a 4-MP electrode (I), an identical electrode modified with 4-MP only (II), and the difference cyclic voltammogram (I–II), which shows only the electrostatically bound 2,6-AQDS²⁻; (c) the capacitance as a function of scan number for a 4-MP-modified Au electrode. All data were obtained in a pH = 2 solution containing 0.2 M phosphate buffer. The 2,6-AQDS²⁻ was preadsorbed by immersion of the 4-MP-modified electrode in 1 mM 2,6-AQDS²⁻ for 5 min. Scan rate was 50 mV/s.

are the scan conditions, the time allotted for monolayer modification, and the time required to achieve saturation coverage of the SAMs by the quinones.

Preliminary data were difficult to interpret because the 2,6-AQDS²⁻_{ads} reduction peak falls near the polarizable limit of the solvent and in certain cases its magnitude is on the order of the capacitive current. We were able to resolve this difficulty by using a pair of matched electrodes: one electrode supported only 4-MP and the other supported both 4-MP and any electrostatically bound 2,6-AQDS²⁻. The two cyclic voltammograms in Figure 2a (I and II) were obtained from electrodes modified with 4-MP only. The difference between the capacitive currents, shown as I–II in Figure 2a, is approximately 5%; this run-to-run variation is typical of several other control experiments.

The cyclic voltammograms shown in Figure 2b correspond to electrodes modified simultaneously with 4-MP (I and II). Electrode I was then immersed in a pH = 2

buffer solution containing 1 mM 2,6-AQDS²⁻ for 5 min, and then it was rinsed with pure buffer solution. The difference (I–II) reflects the voltammetry resulting from 2,6-AQDS²⁻_{ads}. We chose pH = 2 and pH = 7 for these experiments, since we were able to show previously that the surface pK_a for 4-MP = 4.6 ± 0.5 at the potential of zero charge.^{22,23} The voltammetry indicates a chemically reversible and thermodynamically nearly reversible adsorption wave ($\Delta E_p = 30$ mV). The E° value for 2,6-AQDS²⁻_{ads} shifts 70 mV positive of 2,6-AQDS²⁻_{bulk}, which is the same value we observed for 2,6-AQDS²⁻ adsorbed on the naked Au surface. However, the value of $\Gamma_{2,6-AQDS^{2-}}$ is significantly higher on the 4-MP-modified Au surface than on the naked Au electrode as a result of electrostatic binding (0.35×10^{-10} mol/cm² versus 0.13×10^{-10} mol/cm², respectively). The other interesting aspect of Figure 2b is the appearance of a slight difference in the magnitude of the charging current between the Au/4-MP/2,6-AQDS²⁻_{ads} and Au/4-MP-modified electrodes. This result, which we nearly always observe, indicates that the Au/4-MP/2,6-AQDS²⁻_{ads}-modified electrode possesses a higher interfacial capacitance. Similar results have been observed for Au electrodes modified with ferrocene-terminated organomeraptans: capacitance is higher when the ferrocene group is oxidized than when it is in its neutral form.^{24–26} Presumably charge is drawn closer to the electrode in this case, which has the effect of increasing the interfacial capacitance.

The cyclic voltammograms in Figure 2c represent the change in capacitance of a 4-MP-modified electrode as a function of the number of scans, which we recorded sequentially at 30-s intervals (start of the first voltammogram to the start of the following voltammogram) to ensure SAM stability. We observe a similar decrease in capacitance in all experiments where sequential scans are recorded, so we only used data from the first scan to calculate surface coverages. The decrease in capacitance is a rather odd effect since one would anticipate an increase in capacitance if some of the 4-MP monolayer desorbs during voltammetric experiments. Although we do not fully understand this result at the present time, we speculate that each scan results in an improvement in the ordering of the SAM rather than a decrease in stability or organization. Better organized SAMs should maintain liquid-phase ions at longer distances from the Au surface, which will result in lower electrode capacitance. It is also possible that some of the decrease in capacitance arises from surface contamination, but control experiments indicate only a minimal contribution from this channel.

The surface coverage of 2,6-AQDS²⁻_{ads} on the 4-MP surface decreases as a function of time in the 2,6-AQDS²⁻-free buffer solution. To illustrate this change we prepared and analyzed electrodes exactly as described for Figure 2b. Figure 3 is a plot of $\Gamma_{2,6-AQDS^{2-}}$ normalized to the coverage obtained from the first voltammetric wave in the phosphate-buffer solution, as a function of time. The data in Figure 3 indicate a rapid decrease of the surface concentration with scan number: the surface concentration falls to approximately 25% of its original value in 20 min. We ensured that 2,6-AQDS²⁻_{ads}, but not 4-MP, desorbed from the surface by reimmersing the substrate in a 2,6-AQDS²⁻ solution at the end of the desorption

(22) Bryant, M. A.; Crooks, R. M. *Langmuir* **1993**, *9*, 385.

(23) Smith, C. P.; White, H. S. *Langmuir* **1993**, *9*, 1.

(24) Chidsey, C. E. D. *Science* **1991**, *251*, 919.

(25) (a) Delong, H. C.; Donohue, J. L.; Buttry, D. A. *Langmuir* **1991**, *7*, 2196. (b) Delong, H. C.; Buttry, D. A. *Langmuir* **1990**, *6*, 1319.

(26) (a) Rowe, G. K.; Creager, S. E. *Langmuir* **1994**, *10*, 1186. (b)

Creager, S. E.; Rowe, G. K. *Langmuir* **1993**, *9*, 2330. (c) Rowe, G. K.;

Creager, S. E. *Langmuir* **1991**, *7*, 2307. (d) Creager, S. E.; Rowe, G. K.

Anal. Chim. Acta **1991**, *246*, 233.

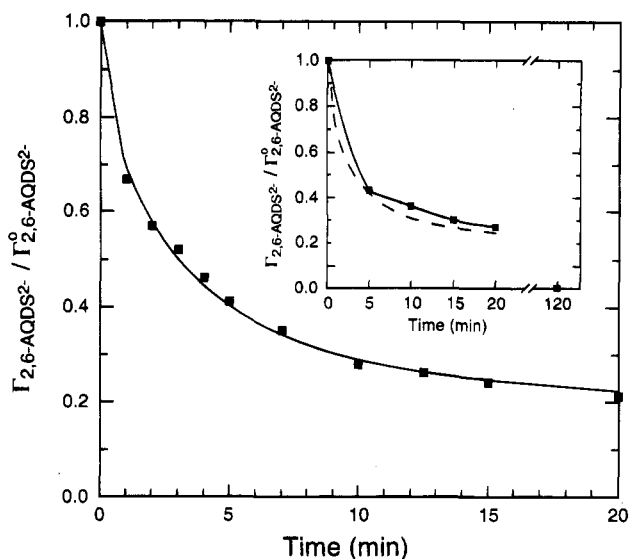


Figure 3. Surface concentration of 2,6-AQDS²⁻ on a 4-MP modified electrode as a function of time. The data were obtained from integrated voltammograms that were recorded sequentially at a rate of 1 voltammogram per minute. The total charge for each voltammogram was normalized to the charge corresponding to the first voltammetric adsorption wave. The inset shows the surface concentration of 2,6-AQDS²⁻ on a 4-MP-modified electrode obtained at 5-min intervals. The data in the main part of the figure are superimposed in the inset (dashed line) to show that desorption is the result only of immersion time rather than the potential scan. The data point at 120 min was obtained independently of the others and shows the 2,6-AQDS²⁻ desorption is complete after this interval. Voltammograms were obtained in a pH = 2, 0.2 M phosphate buffer.

experiment and verifying by cyclic voltammetry that approximately the same amount (85%) of 2,6-AQDS²⁻ that was originally adsorbed to the surface readsorbed.

To determine if desorption is only a function of time, or if it is related to the potential scans, we did a second experiment in which a quinone-modified electrode was scanned at 5 min, rather than 1 min, intervals. Between scans the electrode potential was fixed 200 mV positive of E'' of 2,6-AQDS²⁻_{ads}. The decrease in surface coverage we observed in this experiment is nearly identical to that noted in the experiment where the potential was scanned nearly continuously. We superimposed the data in the large plot (dashed line) over the data shown in the inset to demonstrate the direct correspondence during the first 20 min of the experiment. Since this experiment demonstrates that the quinones start desorbing from the electrode as soon as it is immersed in the buffer, it is critical that the interval between immersion and initiation of the scan be carefully controlled. To determine if a limiting surface coverage of 2,6-AQDS²⁻ is obtained when the Au/4-MP/2,6-AQDS²⁻_{ads} electrode is equilibrated with the 2,6-AQDS²⁻-free buffer solution, we prepared an electrode as before, obtained one cyclic voltammogram to ensure adsorption of the quinone, and then allowed the electrode to stand in the pH = 2 buffer at open circuit for 2 h prior to initiating a second cyclic voltammogram. The experiment revealed no voltammetric wave attributable to 2,6-AQDS²⁻_{ads}.

The final control experiments involved optimization of the 4-MP modification time and the 2,6-AQDS²⁻ soaking time (Figure 4). Figure 4 was generated by soaking a Au electrode in 4-MP for the indicated time interval and then transferring it to a pH = 2, 1 mM 2,6-AQDS²⁻ solution for 5 min prior to determining the peak cathodic current, $i_{p,c}$, which is linearly related to $\Gamma_{2,6-AQDS^{2-}}$. This experiment indicates that complete coverage of the surface by 4-MP

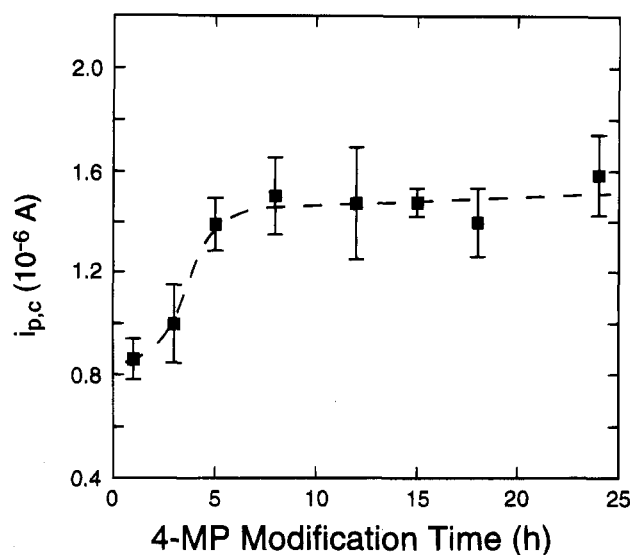


Figure 4. Peak cathodic current ($i_{p,c}$) resulting from the reduction of 2,6-AQDS²⁻_{ads}. Currents were recorded from the first voltammetric adsorption wave as a function of 4-MP modification time to determine optimum electrode preparation conditions. Au wire electrodes were immersed in ethanolic 4-MP solutions for the times indicated and then removed from solution, rinsed with ethanol, immersed for 5 min in 1 mM 2,6-AQDS²⁻, rinsed with pH = 2 buffer, and finally analyzed in probe-molecule-free pH = 2 buffer.

is not achieved for about 7 h, after which there is no further increase in $i_{p,c}$. The error bars represent the range of results we obtained for two independent experiments at each time. On the basis of these data, we selected a 15 h 4-MP modification time for all remaining experiments.

We determined the time necessary to achieve saturation coverage of the 4-MP-modified Au surface with 2,6-AQDS²⁻ by immersing electrodes previously modified with 4-MP for 15 h in a pH = 2 solution of 2,6-AQDS²⁻ for times ranging from 1 to 60 min. However, we were unable to discern a statistical difference in resulting data, and therefore we selected 5 min soaking intervals more for convenience than for any other reason.

We applied the conclusions we drew from these control experiments to the remaining experiments, which involve analysis of the effects of the following parameters on the surface coverage of the probe molecules: (1) bulk-phase probe molecule concentration; (2) ionic strength, buffer pH, and electrolyte counterion; (3) position of the charged site on the SAM molecules.

Effect of the Bulk-Phase Concentration of 2,6-AQDS²⁻ on $\Gamma_{2,6-AQDS^{2-}}$. We examined the relationship between the concentration of the bulk-phase 2,6-AQDS²⁻ soaking solution and $\Gamma_{2,6-AQDS^{2-}}$ on electrodes modified with 4-MP. In most chemical systems, one of two types of surface adsorption processes are operative. In the first case, there is an equilibrium relationship between the bulk-phase and surface-adsorbed concentrations: the surface concentration increases with the bulk-phase concentration according to a thermodynamically reversible adsorption isotherm, such as the Langmuir or Frumkin isotherm. In the second case, the surface concentration is not in equilibrium with the bulk phase and a strong interaction between the adsorbate and the surface results in surface saturation by the adsorbate regardless of bulk-phase concentration. For the molecule/monolayer interactions discussed here, we find that $\Gamma_{2,6-AQDS^{2-}}$ is a function of the bulk concentration of 2,6-AQDS²⁻. The results indicate that the adsorption rate is rapid but that

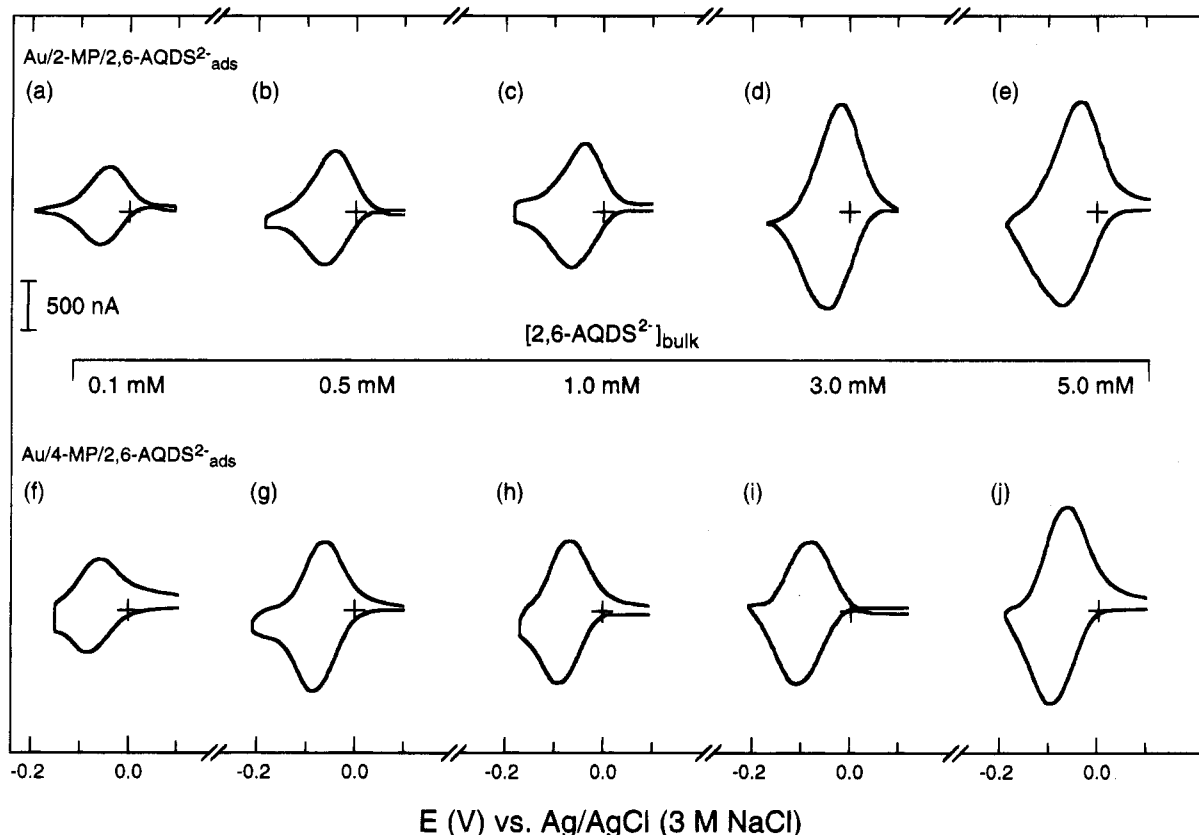


Figure 5. Cyclic voltammetry of 2,6-AQDS²⁻ electrostatically bound to (a–e) 2-mercaptopyridine (2-MP), and (f–j) 4-mercaptopyridine (4-MP) modified Au surfaces as a function of the 2,6-AQDS²⁻ solution concentration used to modify the surfaces. Details of the electrode preparation are given in the text. Voltammograms were obtained in pH = 2, 0.2 M phosphate buffer solutions, and the scan rate was 50 mV/s. All data were recorded on the first voltammetric scan after modification with 2,6-AQDS²⁻.

desorption is relatively slow and therefore the surface is best described as being in slow equilibrium with the bulk solution.

To examine the effect of the bulk-phase concentration of 2,6-AQDS²⁻ on the surface concentration, we soaked 4-MP-modified Au wires in pH = 2 buffer solutions containing different concentrations of 2,6-AQDS²⁻ for 5 min, and then we removed the electrodes, rinsed them in pure buffer solution, and evaluated the surface coverage using the background-subtraction cyclic voltammetric method described earlier. We show the cyclic voltammetric data in the lower part of Figure 5 and the surface concentrations determined from these data in Table 2. The results indicate an increase in $\Gamma_{2,6\text{-AQDS}^{2-}}$ throughout the range 0.1–5.0 mM 2,6-AQDS²⁻, with the steepest part of the adsorption isotherm occurring at the low end of this range. We were not able to exceed 5.0 mM, because that is the approximate saturation concentration of 2,6-AQDS²⁻ in this buffer. Two values for $\Gamma_{2,6\text{-AQDS}^{2-}}$ are provided in Table 2: these were obtained from completely independent experiments and they are included here to emphasize the reproducibility of the experiments.

If we assume that the quinone adsorbs flat onto the Au/4-MP surface, the calculated maximum surface coverage is 1.3×10^{-10} mol/cm².^{20a} This is also the actual coverage measured on naked Pt surfaces that were in contact with 2,6-AQDS²⁻ ranging in concentration from 0.03 to 1.88 mM during the measurement of $\Gamma_{2,6\text{-AQDS}^{2-}}$,^{20b} but it is almost 3 times higher than our measured maximum coverage of 0.45×10^{-10} mol/cm² in 0.2 M phosphate buffer solution. For comparison, a maximum surface concentration of 0.8×10^{-10} mol/cm² has been measured on naked Hg.¹⁶

We can calculate the theoretical maximum ratio of $\Gamma_{4\text{-MP}}/\Gamma_{2,6\text{-AQDS}^{2-}}$ to be approximately 6 by assuming that

Table 2. Surface Coverages of 2,6-AQDS²⁻ on Two Mercaptopyridine-Modified Au Surfaces as a Function of Electrolyte Concentration and the Concentration of 2,6-AQDS²⁻ Used To Modify the SAM Surfaces^a

SAM	$c_{\text{PO}_4^{3-}}$ (M)	$[2,6\text{-AQDS}^{2-}]_{\text{bulk}}$ (mM)	$\Gamma_{2,6\text{-AQDS}^{2-}}$ (10^{-10} mol/cm ²)
Au/4-MP	0.02	0.1	0.36, 0.33
		0.5	0.45, 0.45
		1.0	0.47, 0.45
		3.0	0.48, 0.51
		5.0	0.67, 0.65
	0.20	0.1	0.25, 0.23
		0.5	0.35, 0.33
		1.0	0.35, 0.36
		3.0	0.42, 0.39
		5.0	0.45, 0.40
Au/2-MP	0.02	0.1	0.41, 0.39
		0.5	0.45, 0.41
		1.0	0.49, 0.49
		3.0	0.55, 0.57
		5.0	0.63, 0.61
	0.20	0.1	0.16, 0.15
		0.5	0.24, 0.26
		1.0	0.33, 0.35
		3.0	0.46, 0.44
		5.0	0.47, 0.44

^a Data were obtained in pH = 2 phosphate buffer solutions.

the substrate is primarily of the (111) orientation and that 4-MP adsorbs at 3-fold hollow sites.¹¹ Using the theoretical value of $\Gamma_{4\text{-MP}}$ (7.8×10^{-10} mol/cm²) and the measured maximum value of $\Gamma_{2,6\text{-AQDS}^{2-}}$ in 0.2 M phosphate buffer (0.45×10^{-10} mol/cm²) yields $\Gamma_{4\text{-MP}}/\Gamma_{2,6\text{-AQDS}^{2-}} \approx 17$. Presumably this difference in ratios is primarily due to competition for 4-MP sites by buffer ions: we show in the next section that the maximum in $\Gamma_{2,6\text{-AQDS}^{2-}}$ is a strong function of the buffer concentration. On the basis of

chemical intuition, we believe that a flat orientation of the adsorbate on the SAM surface should be the favored geometry, since it puts both of the negatively charged sulfonate groups in close contact with the positively charged SAM surface. In addition to the strong inclination of these species to ion-pair, which they do in aqueous solutions (precipitation occurs when 1 mM acidic solutions of 4-MP and 2,6-AQDS²⁻ are mixed), this geometry also reduces the magnitude of the positive free energy arising from the close-packed charge of the protonated pyridine surface.^{3d}

It is interesting to speculate on why we measure coverages that are significantly lower than were measured previously on naked metal and carbon surfaces. First, SAMs having ionizable functional groups probably interact with adsorbates differently than nominally naked electrode surfaces. Second, the quinone must displace a more weakly electrostatically bound adsorbate to be present on the surface: this process will be different on a SAM compared to a naked metal surface. One can envision many other differences between the activity and surface free energies of naked and SAM-modified electrodes that could lead to disparate surface coverages. In addition to these chemical phenomena, there are other important considerations that pertain to slight differences in experimental methods between our study and those reported previously. For example, we determine surface coverages in the absence of the adsorbate in the bulk phase, which probably results in the loss of some surface-confined quinone prior to the measurement, while the other studies employed a finite bulk-phase concentration. In addition, we will show later in this paper that the maximum surface coverage is a strong function of the electrolyte concentration: when the phosphate concentration is reduced by an order a magnitude, the $\Gamma_{2,6\text{-AQDS}^{2-}}$ increases by roughly 50% on the 4-MP surface.

Effect of Ionic Strength, Solution pH, and Different Electrolytes on $\Gamma_{2,6\text{-AQDS}^{2-}}$. In this set of experiments, we examined the effect of the total ionic strength of the buffer solution, the solution pH, and several different electrolytes on the surface concentration of 2,6-AQDS²⁻ bound to a Au/4-MP monolayer. We measured the surface concentrations exactly as described in the previous section.⁵

Figure 6 shows voltammetry for pH = 2 phosphate buffer concentrations ($c_{\text{PO}_4^{3-}}$) ranging from 0.02 to 2.0 M. Clearly, the buffer concentration exerts a dramatic effect on $\Gamma_{2,6\text{-AQDS}^{2-}}$. At $c_{\text{PO}_4^{3-}} = 0.02$ M, we observe reduced competition of the electrolyte for surface binding sites and $\Gamma_{2,6\text{-AQDS}^{2-}} = 0.47 \times 10^{-10}$ mol/cm². We obtain a somewhat lower coverage, $\Gamma_{2,6\text{-AQDS}^{2-}} = 0.35 \times 10^{-10}$ mol/cm², when $c_{\text{PO}_4^{3-}} = 0.2$ M, and there is no 2,6-AQDS²⁻ adsorption when $c_{\text{PO}_4^{3-}} = 2.0$ M. Surface coverages measured as a function of $c_{\text{PO}_4^{3-}}$ and the concentration of 2,6-AQDS²⁻_{bulk} are given in Table 2. We observe a similar trend for $\Gamma_{2,6\text{-AQDS}^{2-}}$ on 2-MP-modified electrodes (*vide infra*).

We illustrate the pH dependence of 2,6-AQDS²⁻ binding to a Au/4-MP surface in Figure 7: when the pH of the buffer is high enough to deprotonate the 4-MP SAM, no adsorption of 2,6-AQDS²⁻ occurs. We performed this experiment by modifying two electrodes with 4-MP and soaking one of them (voltammogram I) in a pH = 7, 0.2 M phosphate buffer containing 1 mM 2,6-AQDS²⁻ for 5 min. Subtraction of the two voltammograms (I–II) reveals only a small capacitive current, which probably arises from imperfect subtraction, but no 2,6-AQDS²⁻ adsorption. This observation confirms a critical aspect of the model illustrated in Chart 1: electrostatic binding does not occur unless the 4-MP SAM is protonated.

To further investigate the properties of the unprotonated 4-MP surface, we prepared a series of Au/4-MP/

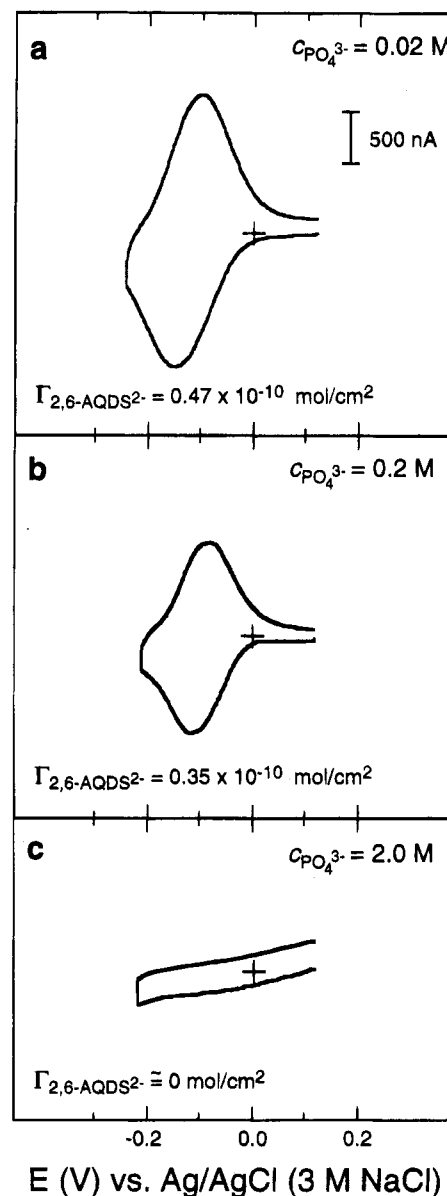


Figure 6. Cyclic voltammetry of 2,6-AQDS²⁻ electrostatically bound to 4-MP-modified Au electrode as a function of phosphate buffer concentration at pH = 2; (a) $c_{\text{PO}_4^{3-}} = 0.02$ M; (b) $c_{\text{PO}_4^{3-}} = 0.2$ M; (c) $c_{\text{PO}_4^{3-}} = 2.0$ M. All data were recorded on the first cyclic voltammetric scan. The resulting surface concentrations are indicated in the figure and details of the electrode preparation are given in the text. Scan rate was 50 mV/s.

2,6-AQDS²⁻_{ads}-modified electrodes in pH = 2 buffer and measured $\Gamma_{2,6\text{-AQDS}^{2-}}$ as a function of the exposure time to pH = 7 buffer solution. The voltammetry shown on the left side of Figure 8 is representative of the first scan in pH = 2 buffer. The electrodes were then removed and placed in a pH = 7, 0.2 M phosphate buffer for 30 s, removed, and returned to the original pH = 2 buffer. The voltammetry shown in the middle column resulted; this process was repeated to yield the voltammetry shown in the right-hand column. The key result is that deprotonation of the 4-MP surface by the pH = 7 buffer rapidly results in desorption of most of the originally adsorbed 2,6-AQDS²⁻.

Figure 9 shows how $\Gamma_{2,6\text{-AQDS}^{2-}}$ varies with pH over the range from 2 to 7. Consistent with the results discussed earlier, we find that the extent of monolayer protonation, which is a function of solution pH,²² determines $\Gamma_{2,6\text{-AQDS}^{2-}}$. At the extreme pH values of 2.0 ($\Gamma_{2,6\text{-AQDS}^{2-}} = (0.47\text{--}0.61) \times 10^{-10}$ mol/cm²) and 6.0 ($\Gamma_{2,6\text{-AQDS}^{2-}} = 0$) we observe limiting

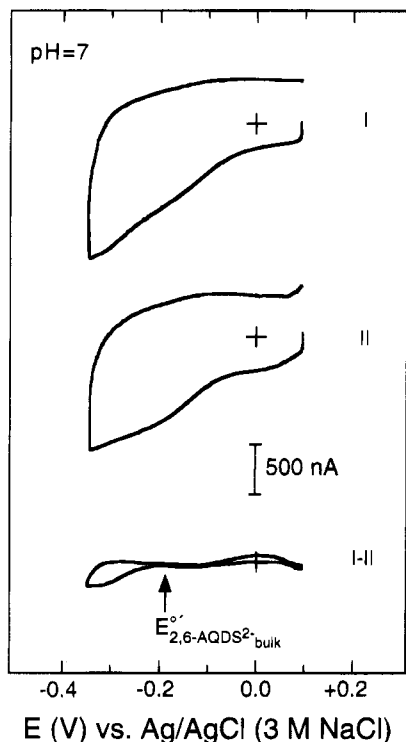


Figure 7. Cyclic voltammetry obtained by (I) immersing a 4-MP-modified electrode in a 1 mM, pH = 7, 2,6-AQDS²⁻ solution for 5 min and rinsing with pH = 7 buffer; (II) 4-MP-modified electrode only; (I-II) difference voltammogram indicating no adsorption of 2,6-AQDS²⁻ onto the 4-MP surface at pH = 7. Data were obtained in a pH = 7, 0.2 M phosphate buffer, at a scan rate of 50 mV/s.

behavior, which we believe reflects complete protonation and deprotonation of the monolayer surface, respectively. At intermediate pH values, intermediate values of $\Gamma_{2,6-AQDS^{2-}}$ obtain. Other experiments at lower pH, which were performed in unbuffered HNO₃ solutions, indicate that $\Gamma_{2,6-AQDS^{2-}}$ is nearly independent of pH at or below pH = 2.

If we ignore activity effects that result from ion-pairing between the monolayer and the probe molecules, we can extract an effective surface pK_a value for the 4-MP monolayer from the data in Figure 9. This value, which is the pH at one-half the maximum surface coverage, is about 4.0. We recently demonstrated an alternative method for measuring the surface pK_a of 4-MP that is based on the pH dependence of the total electrode capacitance.^{22,23} This method yields a surface pK_a value of 4.6 ± 0.5 at 0.2 V (the estimated potential of zero charge) in the absence of specific ion-pairing interactions. Theoretical calculations indicate that in the absence of tautomerism the bulk-phase pK_a of 4-MP would be about 6.^{27,28} We ascribe the small difference between the midtitration point determined using this electrostatic binding method and the pK_a value determined using the capacitance measurement to the substrate potential, which strongly influences the surface pK_a .^{23,29} We made our earlier measurements at 0.2 V, while the adsorption step in the present measurement was done at open circuit. The important point is that there is a smooth transition in the number of protonated sites on the 4-MP surface and that the pH conditions we used to obtain limiting surface coverages (2 and 7) ensure limiting extents of protonation and deprotonation of the 4-MP surface.

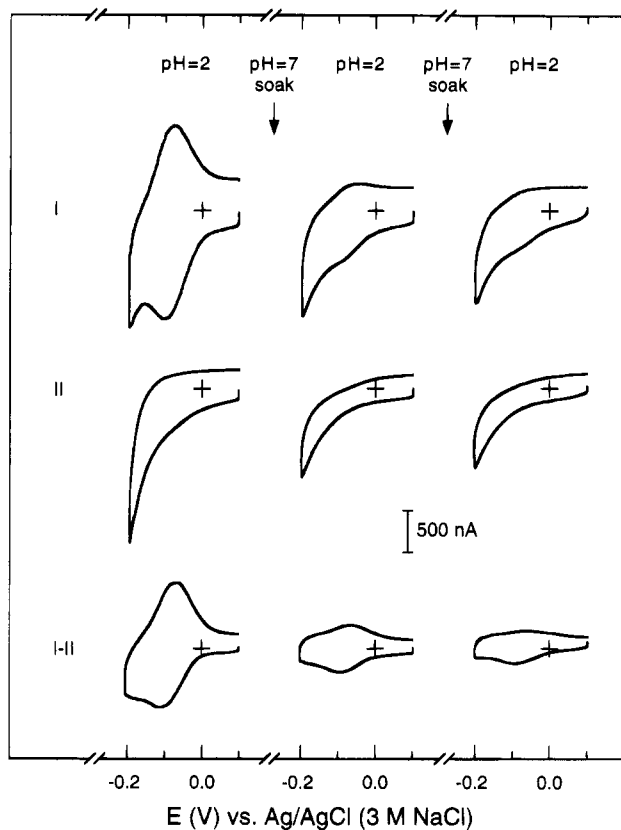


Figure 8. Cyclic voltammetry of (top row) a Au/4-MP/2,6-AQDS²⁻-modified electrode, (middle row) a Au/4-MP-modified electrode, and (bottom row) difference voltammogram (I-II), prepared as described for Figure 2b. The voltammograms on the left were obtained on the first voltammetric scan in pH = 2 phosphate buffer, then the electrodes were immersed in pH = 7 phosphate buffer for 30 s and removed and another set of voltammograms obtained at pH = 2 (middle column). This process was repeated to generate the voltammograms shown in the right-most column. All phosphate buffer solutions were 0.2 M. Initial 2,6-AQDS²⁻ bulk soaking solution was 1 mM. Scan rate was 50 mV/s.

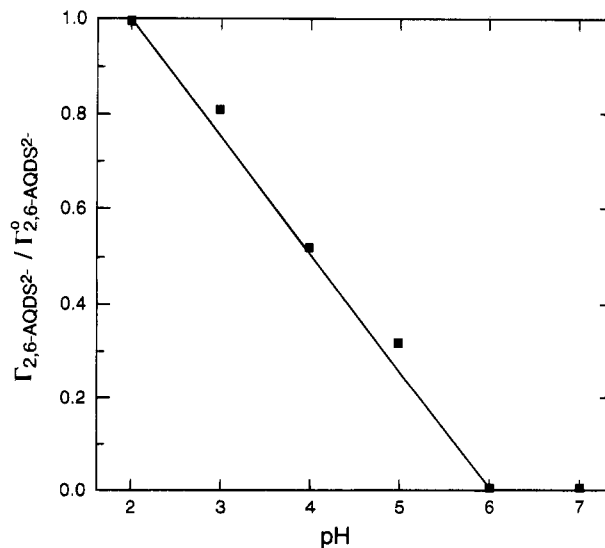


Figure 9. Surface concentration of 2,6-AQDS²⁻ adsorbed onto 4-MP modified electrodes as a function of pH in 0.2 M phosphate buffers normalized to the limiting coverage at pH = 2. The electrode preparation and analysis are described in the text.

(27) Beak, P.; Fry, F. S., Jr.; Lee, J.; Steele, F. *J. Am. Chem. Soc.* **1976**, *98*, 171.

(28) Bock, M. G.; Schlegel, H. B.; Smith, G. M. *J. Org. Chem.* **1981**, *46*, 1925.

(29) Andreu, R.; Fawcett, W. R. *J. Phys. Chem.* **1994**, *98*, 12753.

The change in surface protonation, as reflected by the extent of 2,6-AQDS²⁻ adsorption, changes over a much broader range than for titration of pyridine by a strong

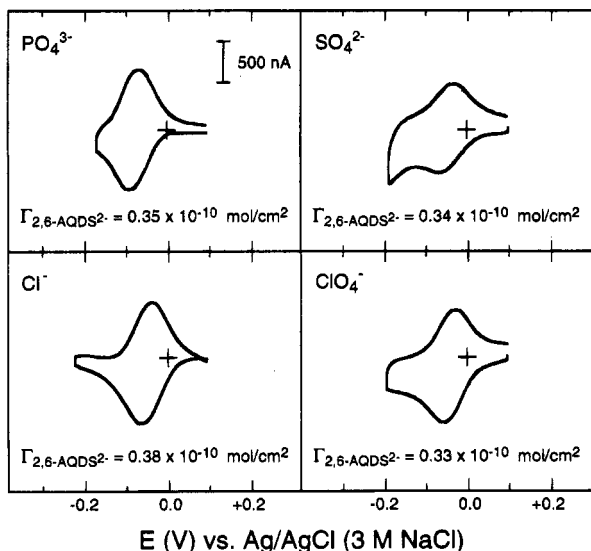


Figure 10. Cyclic voltammetry of Au/4-MP/2,6-AQDS²⁻-modified electrodes, prepared as described for Figure 2b, in 0.2 M, pH = 2 solutions containing the Na⁺ salt of the indicated anion. Scan rate was 50 mV/s.

acid. The 4-MP surface is more than 90% deprotonated over a range of 4 pH units, but in a bulk-phase aqueous solution pyridinium would be 90% deprotonated over a pH range of about 2 pH units. This behavior is predicted theoretically and observed experimentally, and it is rationalized in terms of the progressive difficulty in packing charge onto the surface.^{30,31} In contrast, when the surface concentration of the acid groups is sufficiently dilute, titration curves similar to those observed in the bulk phases are observed.³²

In Figure 10 we show the effect of different types of electrolyte anions on $\Gamma_{2,6-AQDS^{2-}}$ in pH = 2 solutions having a total anion concentration of 0.2 M. We include the results for the phosphate electrolyte (same as Figure 5h) for comparison. There is little difference in $\Gamma_{2,6-AQDS^{2-}}$ or the shapes of the adsorption waves for these four anions. The surface coverage is $(0.35 \pm 0.03) \times 10^{-10}$ mol/cm² and the $E^{o'}$ values are nearly identical, suggesting that the 4-MP/2,6-AQDS²⁻ interaction energy is roughly the same in these three electrolyte solutions. Chemical intuition would suggest that a more highly charged anion, such as SO₄²⁻, might compete more efficiently for 4-MP binding sites, but our experimental results suggest otherwise. Direct comparison is somewhat hindered since the total ionic strengths of these four solutions is not constant. Moreover, the data for the SO₄²⁻ electrolyte solution resulted in imperfect background subtraction. It is also possible that specific chemical interactions between the electrolytes and either 4-MP or 2,6-AQDS²⁻, for example, differences in solubility, exert an equal influence on $\Gamma_{2,6-AQDS^{2-}}$. Regardless of these factors, the total electrolyte concentration and the pH of the solution clearly exert a greater influence over the surface adsorption properties than the chemical nature of the electrolyte ions.

Effect of the Position of the Monolayer Binding Site on $\Gamma_{2,6-AQDS^{2-}}$. In this set of experiments we compared $\Gamma_{2,6-AQDS^{2-}}$ for 4-MP and 2-MP SAMs. We anticipated that $\Gamma_{2,6-AQDS^{2-}}$ would decrease as the charged portion of the monolayer became less accessible to bulk-phase 2,6-AQDS²⁻, but we observed no clear position-dependent trend on $\Gamma_{2,6-AQDS^{2-}}$ for the two mercaptopyridine deriva-

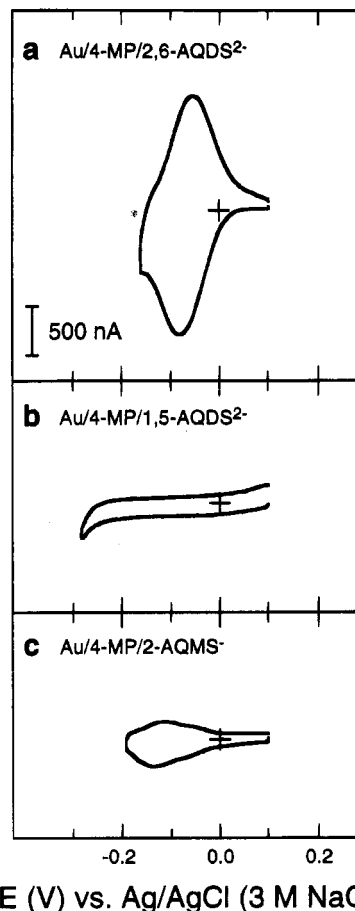


Figure 11. Cyclic voltammetry of anthraquinones adsorbed onto Au/4-MP-modified electrodes as a function of the location and number of sulfonate groups: (a) 2,6-AQDS²⁻; (b) 1,5-AQDS²⁻; (c) 2-AQMS⁻. The scan rate was 50 mV/s. Note that the 1,5-AQDS²⁻ adsorption wave falls negative of the solvent limit and therefore will not be observed even if 1,5-AQDS²⁻ adsorbs to the 4-MP surface.

tives compared in Figure 5 and Table 2. For a particular set of conditions (pH, buffer concentration, and concentration of 2,6-AQDS²⁻_{bulk}) the differences in $\Gamma_{2,6-AQDS^{2-}}$ are statistically indistinguishable. This suggests that at least some of the protonated sites of 2-MP are as accessible to the probe molecules as that of 4-MP.

In contrast to the similar behavior observed at pH = 2 for 4-MP and 2-MP probes, we observe some marked differences at pH = 7. As mentioned previously, we do not observe binding of any 2,6-AQDS²⁻ at pH = 7 on the 4-MP surface, but we do observe a small coverage on the 2-MP surface. This result probably reflects either a higher surface pK_a for 2-MP compared to 4-MP, which means the 2-MP surface is not completely deprotonated at pH = 7 or that there is a driving force for interpenetration of the probe into the SAM even in the absence of a Coulombic interaction. At the present time, we are not able to distinguish between these two possibilities, but we are examining SAMs composed of the three isomers of both aminothiophenol and mercaptobenzoic acid, and we anticipate that the results of this study will be revealing.²

Effect of the Number and Position of Charges on the Probe Molecule on $\Gamma_{2,6-AQDS^{2-}}$. We anticipated that the surface coverage of probe molecules would depend on the number and position of the charged groups on the probe, so we examined the total surface concentration of three different sulfonated anthraquinones on a 4-MP surface (Figure 11). The results indicate that $\Gamma_{2,6-AQDS^{2-}} > \Gamma_{2-AQMS^{-}}$. It is easy to rationalize the low concentration

(30) Mullen, K. I.; Wang, D.; Crane, G.; Carron, K. T. *Anal. Chem.* **1992**, *64*, 930.

(31) Bain, C. D.; Whitesides, G. M. *Langmuir* **1989**, *5*, 1370.

(32) Creager, S. E.; Clark, J. *Langmuir* **1994**, *10*, 3675.

of 2-AQMS⁻ on the 4-MP surface in terms of the total number of binding sites, since we know that a greater number of interaction sites leads to more persistent intermolecular binding interactions.³³ However, we might anticipate a similar degree of electrostatic binding for 1,5-AQDS²⁻ as we found for 2,6-AQDS²⁻ since they both possess two permanent negative charges. Unfortunately, reduction of the electrolyte solution interferes with observation of the 1,5-AQDS²⁻ bulk-phase and adsorption waves. However, the presence of a significant capacitive current in the difference voltammogram may indicate adsorption (compare with the lower voltammograms in Figures 2a and 7 where the capacitive current is essentially zero after subtraction in the absence of adsorption).

Conclusions

We have shown that pH-sensitive SAMs bind suitably charged probe molecules as a function of the bulk-phase pH. This phenomenon is quite general, but the extent to which electrostatic binding occurs depends on several key factors. First, since there is competition for binding sites between the probe molecules and both the solvent and electrolyte, certain favorable conditions must exist. For example, surface binding is enhanced if the probe has limited solubility in water and if it ion-pairs with the SAM to some extent. Second, for the systems discussed here the total surface concentration of the probe is a strong function of the probe and buffer concentrations and the solution pH: electrostatic binding is favored on highly charged SAMs in low-ionic-strength solutions. Finally,

the nature of the probe molecule is important. Probes with two negative charges bind strongly to 4-MP, but a much weaker interaction is observed for the singly-charged probes even though it is less soluble in water. Others have taken advantage of multiple-point binding to design highly stable electrostatically bound ionomer layers.^{8,9}

In our first report of electrostatic binding to SAMs, we indicated that after a few voltammetric scans roughly half of the adsorbed probe remained on the 4-ATP SAM surface, but in experiments discussed here we find that only 25% of the initially adsorbed SAM remains after 20 min, and none is detectable after 2 h. Clearly this approach for interfacial design has some important limitations: lack of long-term stability in this case. However, this can be a significant advantage in certain applications, such as chemical sensing, where it is essential that the surface concentration be related to the bulk-phase concentration according to an equilibrium isotherm.

We are continuing our study of electrostatic binding phenomena by examining different types of monolayer surfaces, electrode potential effects, adsorption geometries, and other fundamental relevant factors. In addition, we are just beginning to examine competitive binding and chemical and biochemical sensing applications that rely upon electrostatic interactions between monolayers and molecules.

Acknowledgment. We gratefully acknowledge the National Science Foundation (CHE-9313441) for full support of this research. We also acknowledge helpful discussions with Professor Li Sun (University of Minnesota).

LA940669H

(33) Kurihara, K.; Ohto, K.; Honda, Y.; Kunitake, T. *J. Am. Chem. Soc.* **1991**, *113*, 5077.